

LIQUID COMPOSITE MOULDING: INFLUENCE OF FLOW FRONT CONFLUENCE ANGLE ON LAMINATE POROSITY

Gion A. Barandun, Paolo Ermanni

Centre of Structure Technologies, ETH Zurich, Leonhardstrasse 27, 8092 Zurich, Switzerland: gbarandun@ethz.ch

ABSTRACT: Advanced Liquid Composite Moulding processes using injection strategies with multiple gates often lead to unwanted filling patterns. Simulation and optimization can contribute to further enhance the filling process; nevertheless flow front confluences (weld lines) cannot be completely avoided. This paper presents the results of a study aiming at the investigation of the relationship between the confluence angle and the local laminate quality of the impregnated part. Part quality has been determined based on the porosity in the confluence zones and in the undisturbed part zones. A total of 108 specimens has been evaluated. Micrographic image processing has been done automatically by software to guarantee constant conditions for every image. Additionally, to globally visualize porosity, some parts have been processed using transmitted light and thermography. These inquiries allow a qualitative conclusion on the laminate structure and thus the porosity of the produced parts.

The micrographic image processing clearly shows that porosity is significantly higher in the confluence area, depending on the confluence angle. An angle of 20° (measured between the flow directions) leads to a porosity increase of approx. 1.5%, whereas an angle of 160° already increases the porosity more than 4%.

KEYWORDS: Liquid Composite Moulding, Part Quality, Porosity, Flow front confluence, Confluence Angle, Weld line, Micrographic image processing.

INTRODUCTION

A variety of commercially available process simulation tools are used to support the development of Liquid Composite Moulding parts [1, 2]. In this context, LCM process optimization using Evolutionary Algorithms is an actual research topic [3-5]. Objective functions include filling time, fill grade and criteria related to laminate quality, one of them being the angle between two colliding flow fronts. As a worst case scenario, two flow fronts joining with an angle of 180° (“head-on”) will form voids, as either the entrapped air cannot move towards a vent or, in case of vacuum assisted injection, areas with dry or not completely impregnated fibres might be generated. Those effects are occurring at angles below 180°, although in alleviated manner. This paper presents an experimental investigation targeting the quantification of the impact of the confluence angle on the porosity of the final part. Several samples are produced and then analysed by micrographic images.

EXPERIMENTAL PROGRAMME

The different confluence geometries are illustrated in Fig. 1. Samples have been manufactured in a glass tool, to be able to monitor flow front progression. Two symmetrically placed injection ports fill the form building a confluence zone between the two linear flow fronts. For this study, a biaxial ($\pm 45^\circ$) fabric from COTECH in conjunction with the SIKA Biresin L84T epoxy resin system were used. The resin was injected at 60°C (resin viscosity $60\text{mPa}\cdot\text{s}$) with a constant pressure of 2 bar. 12 fibre layers were stacked into the cavity (height 5mm), resulting in a fibre volume content of 40.6%. As soon as complete cavity had been reached, the injection gates were closed.

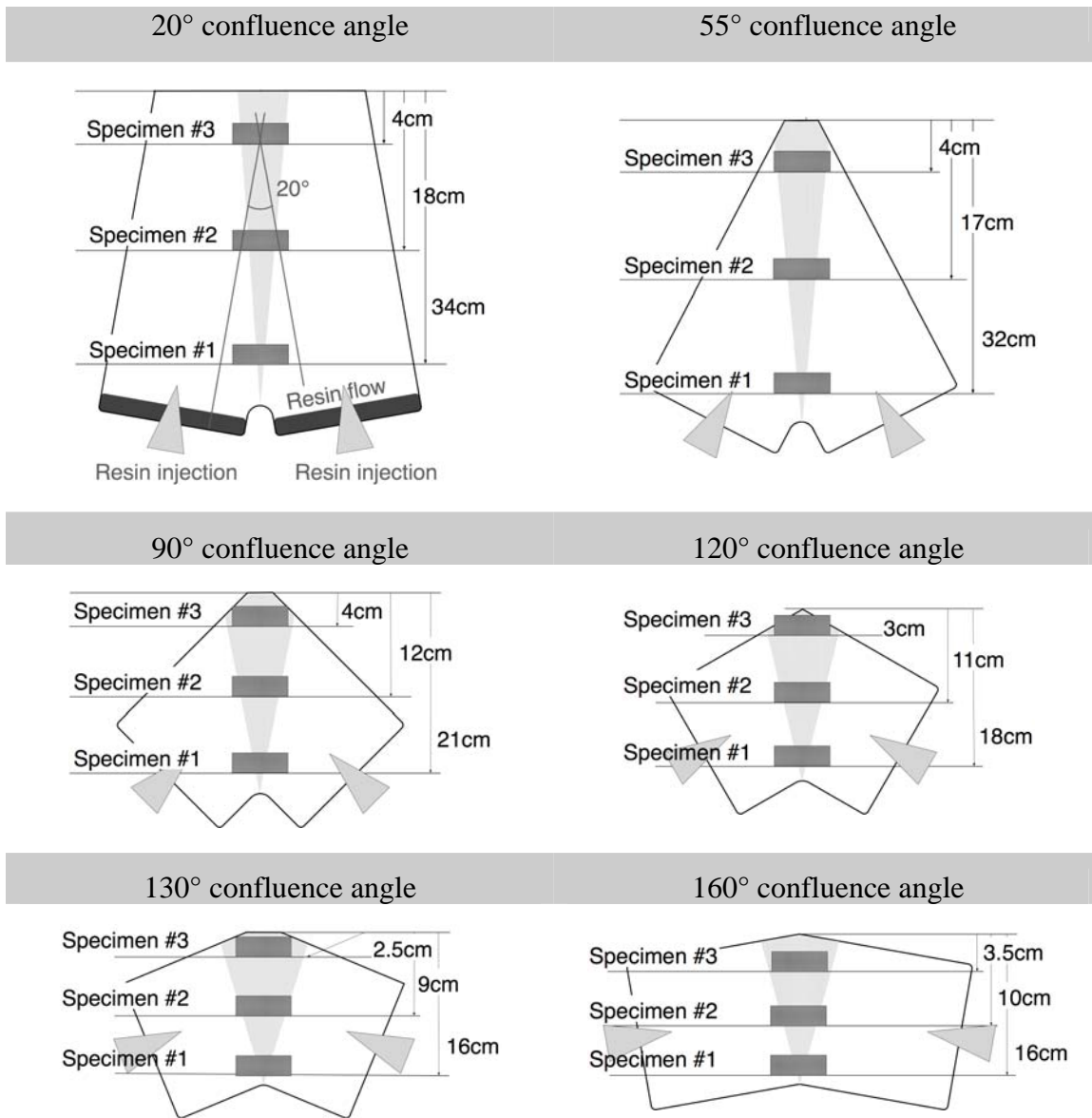


Fig. 1 Sample parts

The specimens for micrographic analysis were cut out from the sample parts as illustrated in Fig. 1. The image layer is always in flow direction, as shown in Fig. 2. The fibre orientation is the same in all images. As the fabric is isotropic, the flow direction has no influence on void formation.

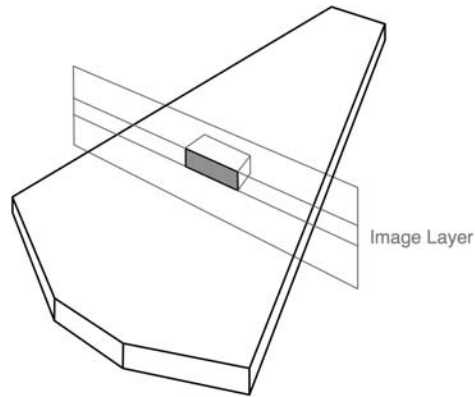


Fig. 2 Specimen orientation

RESULTS

Table 1 and Table 2 show the porosity values for the samples in the confluence and in the undisturbed zone respectively. Average values are summarized in Table 3. Three experiments were carried out for every confluence angle. Fig. 3 shows a micrograph of a laminate produced with confluence angle 55°. On the left hand side, the original picture can be seen. The right hand side shows the corresponding binary picture (entrappings marked in black) including the measurement frame and the scale. The frame is chosen in a way that takes into account the inevitable shading of the picture in the corners.

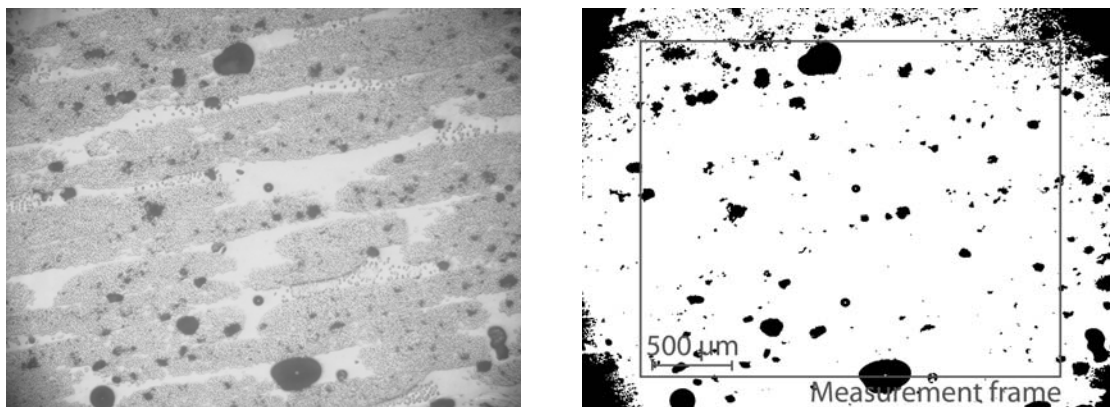


Fig. 3 Micrographic image of 55° sample. Right hand side picture shows binary representation for image data processing

Cutting samples were taken at three different positions in the confluence zone (Fig. 1). To be able to better quantify the effect of the flow front confluence, additional specimens have been cut out from undisturbed part zones. The values obtained were used as a reference to exclude

effects not directly related to flow confluence. As shown in Fig. 4 the porosity increases with increasing confluence angle.

Table 1 Porosity in confluence zone determined by micrographic image processing

		Angles	20°	55°	90°	120°	135°	160°	
Porosity	Exp. #1	Spec. #1	1.46%	4.86%	n.a.	6.76%	5.70%	3.97%	
		Spec. #2	3.03%	5.37%	n.a.	2.99%	4.81%	5.72%	
		Spec. #3	3.58%	5.76%	n.a.	6.97%	4.86%	5.58%	
	Exp. #2	Spec. #1	2.22%	3.28%	5.85%	4.12%	4.82%	8.87%	
		Spec. #2	4.63%	3.35%	4.43%	4.09%	4.61%	7.56%	
		Spec. #3	2.39%	4.22%	3.42%	5.28%	4.62%	5.99%	
	Exp. #3	Spec. #1	1.69%	5.35%	6.6%	6.94%	8.70%	n.a.	
		Spec. #2	4.90%	2.90%	6.34%	6.28%	5.15%	n.a.	
		Spec. #3	2.87%	7.37%	6.25%	10.22%	5.82%	n.a.	
	Mean value			2.97%	4.72%	5.48%	5.96%	5.45%	6.28%

Table 2 Porosity in undisturbed part zones

		Angles	20°	55°	90°	120°	135°	160°	
Porosity	Exp. #1	Spec. #1	n.a.	1.43%	n.a.	2.98%	1.36%	1.04%	
		Spec. #2	n.a.	2.11%	n.a.	2.69%	2.12%	1.19%	
		Spec. #3	1.99%	3.20%	n.a.	2.28%	2.60%	3.05%	
		Spec. #4	1.36%	3.52%	n.a.				
	Exp. #2	Spec. #1	1.15%	0.37%	n.a.	1.51%	0.54%	1.77%	
		Spec. #2	0.97%	1.65%	n.a.	1.84%	1.29%	1.88%	
		Spec. #3	1.79%	2.62%	n.a.	2.13%	2.10%	2.14%	
		Spec. #4	1.50%	2.01%	n.a.				
	Exp. #3	Spec. #1	0.32%	2.40%	2.32%	3.41%	1.52%	3.20%	
		Spec. #2	1.76%	2.93%	2.67%	2.55%	1.63%	2.75%	
		Spec. #3	1.18%	1.52%	2.19%	2.33%	1.55%	2.78%	
		Spec. #4	1.59%	2.72%	n.a.				
	Mean value			1.36%	2.21%	2.39%	2.41%	1.63%	2.20%

Table 3 Summary: Porosity due to flow front confluence

Angles	20°	55°	90°	120°	135°	160°
Total porosity	2.97%	4.72%	5.48%	5.96%	5.45%	6.28%
Basic porosity	1.36%	2.21%	2.39%	2.41%	1.63%	2.20%
Porosity due to confluence	1.61%	2.51%	3.09%	3.55%	3.82%	4.08%

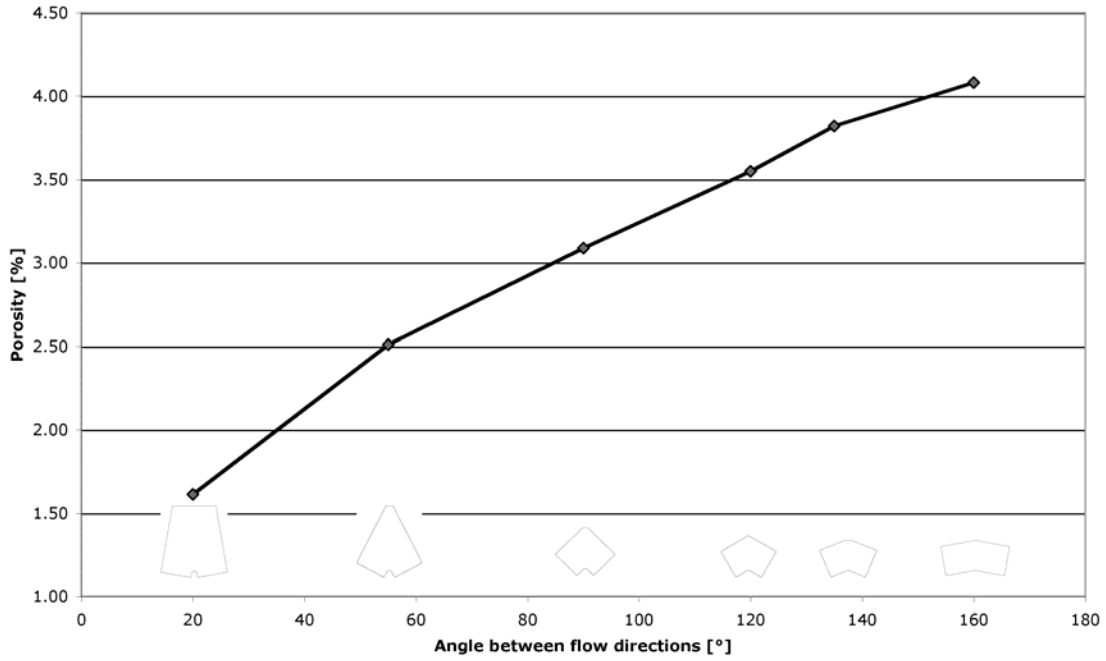


Fig. 4 Relative porosity vs. confluence angle

It seems that the effect of the confluence angle on porosity is reducing with angles above 60° (Fig. 5). As the basic porosity is about 2% for all measured samples, the porosity caused by the confluence rises from values below 2% for an angle of 20° up to 4% for an angle of 160°.

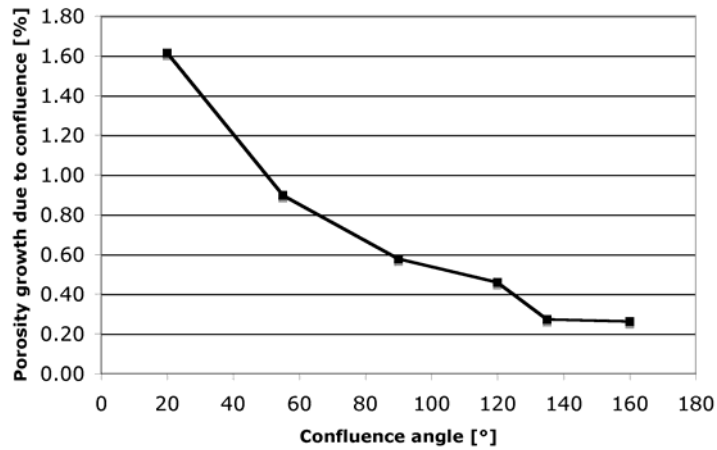


Fig. 5 Porosity growth rate vs. confluence angle. With increasing angle, the effect of the confluence diminishes

Evaluation of global porosity

Micrographics analysis only provides punctual information about laminate porosity. To obtain a global estimation of the porosity, images using transmitted light were produced for the parts with confluence angles of 55° and 160°. For this purpose, the laminates were placed into the manufacturing frame, as shown in Fig. 6, left hand side, laid on a light table and photographed with a digital camera. In undisturbed zones, the light is transmitted smoothly

through the part, whereas in the confluence zones, the light is scattered on the entrapped air, thus this zone appears darker than the rest. Fig. 6 shows the results for the 160° laminate. The confluence zone can be seen without magnification, as a darker area in the middle of the part, whereas for smaller angles it is more difficult to visualize the confluence zone.

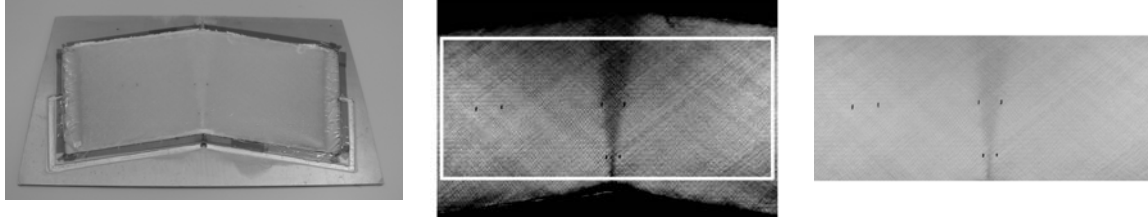
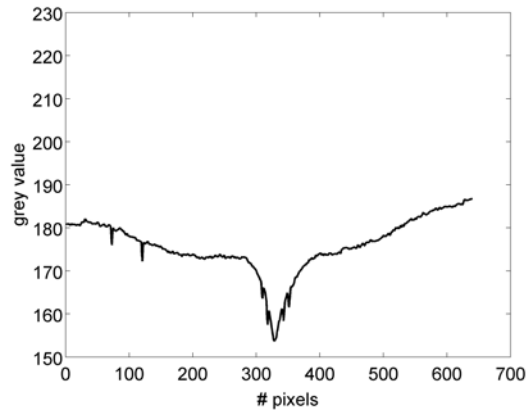
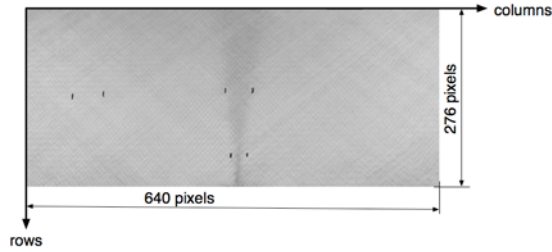


Fig. 6 Sample data processing using transmitted light: The area of interest is marked by the frame (middle image). The darker area resulting from the joining flow fronts is clearly visible

Data processing was performed using Matlab. The color image was first converted in a greyscale image (using Adobe Photoshop). The interesting zone was then cut out for data analysis (Fig. 6, right hand side). Matlab reads the image as matrix of grey values and thus allows analysis of intensity values over every row and column, as well as calculation of mean values for rows or columns. 0 stands for pure black and 255 for pure white. Fig. 7 shows the photograph and the horizontal mean intensity for the 160° and 55° sample, respectively.

The 55° sample is generally brighter; this is not only a result of better impregnation (due to the longer flow path and thus better wetting), but also due to white balance from camera software, because the 55° sample is bigger than the 160° sample. On both samples, the intensity increases toward the injection ports. This is in accordance to several sources [6, 7], stating worse part quality in the zone near the vents. However, to be able to correlate intensity values to porosity content, a wider range of images would be required, and the photographs would have to be taken in a dark room using RAW format, as this prevents any automatic image correction and white balance.

Confluence angle 160°



Confluence angle 55°

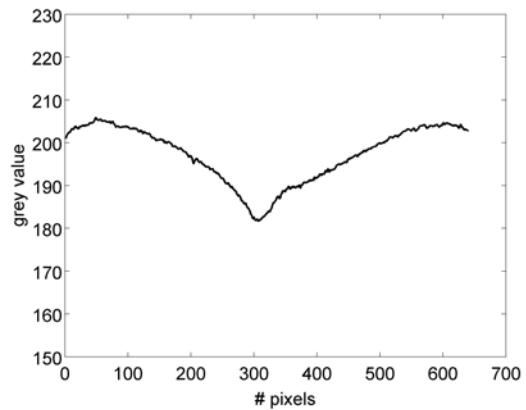
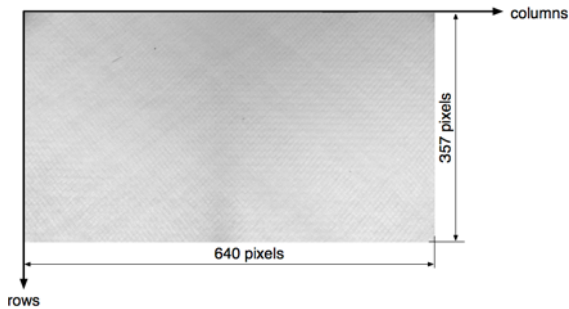


Fig. 7 Image processing using transmitted light: mean of grey value vs. image height

CONCLUSIONS

The results of this study have highlighted the influence of flow front confluences on the laminate porosity. This parameter needs to be taken into account during process development. In order to achieve optimum laminate quality, suitable filling patterns should have as few confluences as possible. In any case, the angle between the joining flow fronts should not exceed 60°. These results are particularly important for injection processes using multiple gates.

As a next step we plan to implement the results of this study in FELyX [8], our simulation and optimization software. Confluence length and angle will be included in the objective function of the Evolutionary Algorithm.

ACKNOWLEDGMENTS

The authors gratefully acknowledge the support by Alcan Technology & Management Ltd.

REFERENCES

1. P. J. C. Serrano, U. K. Vaidya, „Modeling and implementation of VARTM for civil engineering applications“, *SAMPE Journal*, Volume 41, no. 1, Pages 20–31, (2005).
2. M. Henne, C. Leppin, C. Gotschi, „Isothermal RTM simulation of GFRP parts for automotive applications“, *Proc. of International SAMPE Symposium and Exhibition*, Volume 46, Pages 35–347, (2001).
3. P. Simacek, S. G. Advani, „Desirable Features in Mold Filling Simulations for Liquid Composite Molding Processes“, *Polymer Composites*, Volume 25, no. 4, Pages 355-367 (2004).
4. G. A. Barandun, U. Fasel, J. S. U. Schell, P. Ermanni, „Development of an Optimization and Tool for LCM Processes using Evolutionary Algorithms“, *Advancing with Composites*, Milan, Pages 111–117 (2003).
5. B. Y. Kim, G. J. Nam, J. W. Lee, „Optimization of Filling Process in RTM using a Genetic Algorithm and Experimental Design Method“, *Polymer Composites*, Volume 23, no. 1, Pages 72-86 (2002).
6. J. Feuerlein, „Determination of the optimal flowfront-velocity“, *Semester Thesis 02-29, Centre of Structure Technologies, ETH Zurich* (2002).
7. T. S. Lundström, B. R. Gebart, C. Y. Lundemo, „Void formation in RTM“, *Journal of Reinforced Plastics and Composites*, Volume 12, Pages 1339–1349 (1993).
8. O. König, M. Wintermantel, N. Zender, „FELyX - The Finite Element Library eXperiment“, *Tech. rep., Centre of Structure Technologies, ETH Zurich* (2002).
URL <http://felix.sourceforge.net/downloads/FELyX-Paper.pdf>